Research Article | Vol. 10, No. 12 / 1 December 2019 / Biomedical Optics Express 6580
Biomedical Optics EXPRESS

Infrared inhibition and waveform modulation of action potentials in the crayfish motor axon

XUEDONG ZHU,[1,2,5] JEN-WEI LIN,[3] AND MICHELLE Y. SANDER[2,4,5,6,*]

[1]*Department of Biomedical Engineering, Boston University, 44 Cummington Mall, Boston, MA 02215, USA*
[2]*Neurophotonics Center, Boston University, 24 Cummington Mall, Boston, MA 02215, USA*
[3]*Department of Biology, Boston University, 5 Cummington Mall, Boston, MA 02215, USA*
[4]*Department of Electrical and Computer Engineering, Boston University, 8 Saint Mary's Street, Boston, MA 02215, USA*
[5]*Photonics Center, Boston University, 8 Saint Mary's Street, Boston, MA 02215, USA*
[6]*Division of Materials Science and Engineering, Boston University, 15 Saint Mary's Street, Brookline, MA 02446, USA*
[*]*msander@bu.edu*

Abstract: The infrared (IR) inhibition of axonal activities in the crayfish neuromuscular preparation is studied using 2 μm IR light pulses with varying durations. The intracellular neuronal activities are monitored with two-electrode current clamp, while the IR-induced temperature changes are measured by the open patch technique simultaneously. It is demonstrated that the IR pulses can reversibly shape or block locally initiated action potentials. Suppression of the AP amplitude and duration and decrease in axonal excitability by IR pulses are quantitatively analyzed. While the AP amplitude and duration decrease similarly during IR illumination, it is discovered that the recovery of the AP duration after the IR pulses is slower than that of the AP amplitude. An IR-induced decrease in the input resistance (8.8%) is detected and discussed together with the temperature dependent changes in channel kinetics as contributing factors for the inhibition reported here.

1. Introduction

Modulation of neural and muscular activity is essential for both basic research and clinical applications. While implantable electrodes for electrical stimulation have been developed as heart pacemakers, hearing implants and deep brain stimulators, pulsed IR light has recently shown promise as an alternative modality for nerve and muscle stimulation [1–7]. Potential advantages of infrared stimulation over electric stimulation include high spatiotemporal precision, non-invasiveness and contact-free delivery [5,8]. However, the underlying biophysical mechanisms and the intricate interplay of various contributing factors to infrared nerve interactions remain an interesting research field. It has been suggested that thermal transients induced by water absorption of pulsed IR light could be the underlying mechanism for neuronal excitation [9]. Changes in the membrane capacitance caused by spatiotemporal temperature gradients have been demonstrated to depolarize cells and elicit action potentials [10–13]. Pulsed IR light irradiation has also been shown to modulate intracellular calcium dynamics in neonatal ventricular cardiomyocytes [14], in astrocytes and neurons *in vivo* [15], and in spiral and vestibular ganglion neurons [16]. Other postulated mechanisms associated with IR stimulation include the activation of temperature sensitive ion channels [17], the formation of nanopores in the plasma membrane [18], and optoacoustic effects resulting from nanosecond laser pulse stimulation [19,20]. Depending on the stimulation parameters, the cell physiology and the structure of the biological systems studied, different biophysical mechanisms have been shown to be dominant.

#378271 https://doi.org/10.1364/BOE.10.006580
Journal © 2019 Received 20 Sep 2019; revised 12 Nov 2019; accepted 19 Nov 2019; published 27 Nov 2019

Biomedical Optics EXPRESS

In addition to IR neural stimulation, suppression of neural activities and blocking of action potentials by pulsed IR light have also been reported in both *in vivo* and *in vitro* studies [21–31]. IR neural inhibition effects were observed during several IR nerve stimulation studies in both the central [22,24] and the peripheral [23, 31] nerve system. These studies, though mainly focused on the stimulation, raised the question whether IR pulses could be used to inhibit neural activities, and what biophysical mechanisms would contribute to this phenomenon. However, the extracellular recordings used in the studies with the central nerve system could not differentiate whether the inhibition was the result of exciting inhibitory neurons or due to direct suppressive effects. In fact, IR irradiation has been shown to enhance the GABA neurotransmitter release in cultured rat cortical neurons [21]. The IR mediated inhibition has been investigated in diverse preparations and under different experimental conditions. A study showed that IR pulses could block the AP propagation in both the unmyelinated *Aplysia* nerve and the myelinated rat sciatic nerve [25]. Reversible blocking of cultured hippocampal neuron firing [26] and arresting of cardiac contractions in embryonic avian hearts [27] were also reported. It was further demonstrated that a certain degree of fine control in IR mediated inhibition is possible. For example, it was demonstrated that IR pulses could preferentially inhibit small-diameter axons at low radiant exposures [28]. A simulation study of combined thermoelectric stimulation suggested that the threshold for generating compound action potentials (CAPs) with electrical stimulation increased with the increase of the local temperature induced by IR light and that the blocking of AP generation required a lower temperature rise compared to the blocking of propagating APs [32].

Though it is understood that IR inhibition and stimulation both rely on photothermal effects, the underlying biophysical mechanisms and detailed dynamics still remain to be unified. It has been demonstrated that the ambient temperature changes can affect ion channel kinetics and membrane permeability [33,34]. The thermal inhibition hypothesis thus has been proposed, which suggests that the temperature rise induced by IR pulses can alter the membrane properties and ion channel kinetics such that the neural excitability is inhibited [25,28,32,35]. However, most of the experimental IR nerve inhibition studies so far either monitored the all-or-none aspect of neuronal activities by using extracellular recordings or imaging techniques. Observing the intracellular and subthreshold events induced by IR pulses will thus advance our mechanistic interpretation of IR mediated inhibition.

In this paper, the unmyelinated motor axons of the crayfish opener preparations are used to examine the intracellular events associated with IR induced inhibition. This preparation allows simultaneous monitoring of the important parameters for IR mediated neuronal modulation, namely the subthreshold membrane potential, the action potential waveform, the input resistance and the temperature transients during and after IR irradiation. Thus, the inhibition effects of IR pulses captured in this context are for the first time based on intracellular axonal recordings with high resolution and combined with a quantitative analysis. For our studies, the motor axon is locally illuminated by 2 μm IR square pulses delivered with a 50 μm fiber core. The reported results based on intracellular recordings fill the information gap among existing literatures and provide insights into the mechanisms and dynamics of IR induced inhibition.

2. Materials and methods

2.1. Preparation and electrophysiological recording

Crayfish (*Procambarus clarkii*) of both sexes were purchased from Niles Biological Supplies (Sacramento, CA). The opener neuromuscular preparation from the first walking leg was dissected in physiological saline containing (mM): 195 NaCl, 5.4 KCl, 13.5 $CaCl_2$, 2.6 $MgCl_2$, 10 HEPES (pH 7.4). The upper shell of the carpopodite was removed after the leg was glued (Krazy Glue, NC, USA) dactylopodite side down to a 35 mm petri dish (Fig. 1(a)). Only the inhibitory motor axon (~30 μm in diameter) was used in this study. The saline was circulated by a peristaltic pump (Gilson Minipuls 2, Middleton, WI, USA) at a rate of 1.5 ml/min. Due to variations among

Biomedical Optics EXPRESS

preparations, some crayfish axons exhibited strong accommodation such that the AP firing only appeared for about 100 ms at the beginning of the suprathreshold current injection steps. In order to obtain a consistent and stable AP firing during the entire current step period of 1 to 1.5 s, 4-aminopyridine (4-AP) at 200 μM was used in most preparations to block low threshold 4-AP sensitive K^+ channels in this report [36]. Recordings were started ~20 minutes after 4-AP was added, to ensure steady levels of blockage. The IR inhibition effects on AP firing were similar with and without 4-AP. All chemicals were purchased from Sigma-Aldrich.

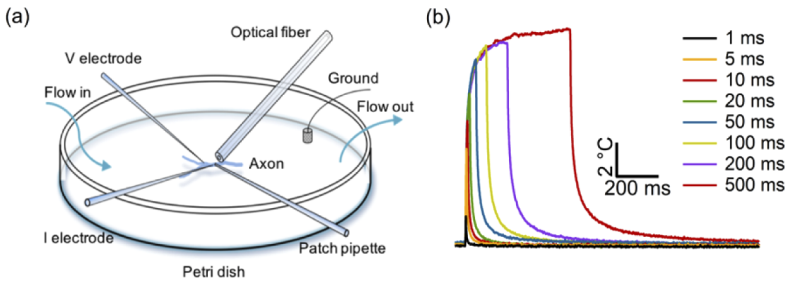

Fig. 1. Illustration of the experimental configuration and recorded temperature transients. (a) The crayfish opener neuromuscular preparation was glued to the bottom of the Petri dish. The current injection electrode (I electrode) used to elicit APs was located closer to the primary branch of the inhibitory axon and the voltage recording electrode (V electrode) was placed ~200 μm to 300 μm distal to the branching point. An optical fiber with a 50 μm core diameter tilted at an angle of ~28° to the horizontal plane delivers infrared light. The tip of an open patch pipette was placed close to the axon and I electrode in the illuminated area. (b) Representative temperature transients converted from the open patch pipette recordings. IR pulse durations varied from 1 ms to 500 ms, from left to right, which resulted in temperature changes between 2 to 12°C.

Two-electrode current clamp (TECC) was performed with AXOCLAMP-2A (Axon Instruments Inc., CA, USA) and IE201 (Warner Instrument Corp., CT, USA). Current steps, –10 nA to 30 nA in amplitude and 1 to 1.5 s in duration, were injected intracellularly to elicit axonal activities. Voltage signals were filtered at 5 kHz and sampled at 50 kHz (NI USB 6361). Microelectrodes with 40–60 MΩ resistance were filled with 500 mM KCl for axonal recording. For our experimental setup configuration depicted in Fig. 1(a), the IR illumination did not generate any detectable potential changes when the voltage recording electrode was immersed in the saline bath before penetrating the axonal membrane.

For the electrophysiology recordings, two axonal electrodes were placed near the primary branch in a distal-to-proximal direction. The open patch pipette for temperature monitoring and the optical fiber for light delivery approached the preparation from opposite directions (Fig. 1(a)). The four elements were arranged with an angle of ~28° to the horizontal plane. For an optimized alignment, the optical fiber was first lowered to touch the surface of the axon before it was raised slightly. The light of a red laser diode was coupled into the optical fiber to facilitate the alignment of the invisible infrared laser beam so that the current injection electrode could be positioned within close proximity of the illuminated spot. The tip of the patch pipette was positioned at the center of the illuminated area, near the current injection electrode. Axon penetration and placement of the optical fiber and patch electrode were performed under an Olympus 60X water immersion lens.

2.2. *Infrared laser light configuration*

A fiber-coupled diode laser (FPL2000S, Thorlabs) with a wavelength centered at 1994 nm with a 3-dB linewidth of 3.6 nm was used as the illumination source for the IR inhibition experiments.

Biomedical Optics EXPRESS

The delivery fiber with a core diameter of 50 µm was cleaned and cleaved before each experiment and positioned slightly above the axon surface at an angle of 28° to the horizontal plane. Single IR square pulses with varying durations (20–500 ms) were used in this report. The output power was measured at the delivery end of the fiber pigtail and kept constant at 7.1 mW. The energy for the 20 ms and 500 ms pulse corresponded to 0.142 mJ and 3.55 mJ, respectively. Due to water absorption (absorption coefficient of 73.9 cm^{-1} for 1994 nm light) [37], the energy that reached the surface plane of the axon was reduced to around 42% of the energy at the optical fiber tip. Based on an estimated distance between the axon surface and the fiber tip of ~ 120 µm, the illuminated area covered ~4200 μm^2 so that the resulting fluence on the surface of the axon was estimated to be about 0.44 J/cm^2 – 11.38 J/cm^2. The output power and duration of the IR square pulses were modulated by an Igor Pro (WaveMetrics) software interface and a data acquisition platform (NI USB 6221). The onset of the IR pulse was delayed with regards to the current injection to the axon by an offset of 100 ms.

2.3. Temperature recording

An open patch pipette, filled with physiological saline, ~5 MΩ in resistance, was used to monitor temperature changes induced by the IR illumination [38]. The patch pipette featured an opening of approximately 1 µm at the tip and the illuminated section contained < 1 µl saline. The Ag/AgCl metal wire was 3–4 cm away from the illuminated spot, which was ~50 µm × 100 µm. To record the temperature changes with a patch pipette, the activation energy of the saline solution was first determined. The patch pipette was immersed into the recording petri dish filled with saline. The perfusion tubing for circulating the saline was fixed to a Peltier coupled copper plate to heat or cool the saline entering the recording petri dish. The bath temperature was monitored with a thermometer (BAT-12, Physitemp Instruments). As the saline temperature was changed from 283.2 K to 316.2 K, voltage clamp currents in response to +5 mV to + 15 mV step commands were measured. The natural logarithm applied to the Arrhenius equation (Eq. (1)) was used to derive the activation energy (E_a) of the saline:

$$\ln(I) = \frac{E_a}{R}\frac{1}{T_0} + \ln(I_0) - \frac{E_a}{R}\frac{1}{T} \tag{1}$$

Here, T is the saline temperature in Kelvin; I is the step current at each corresponding temperature T; T_0 is the room temperature; I_0 is the current step recorded at T_0; and R is the gas constant. The averaged E_a for the saline solution was 3.7 ± 0.08 kcal mol^{-1} (mean ±SEM, $N = 5$), which is comparable to the value 3.84 kcal mol^{-1} found in literature [38]. This was then used to calculate the IR induced temperature transients according to Eq. (2). During the axonal

$$T = \frac{1}{\frac{1}{T_0} - \frac{R}{E_a}\ln\left(\frac{I}{I_0}\right)} \tag{2}$$

recordings, the temperature monitoring pipette tip was positioned right above the axon close to the current injection electrode and the center of the IR illumination. Representative temperature transients caused by a series of square IR pulses are shown in Fig. 1(b). The IR power was maintained at 7.1 mW with durations varying from 1 ms up to 500 ms. The temperature rise varied between 2 °C (1 ms) to 12 °C (500 ms) and reached a plateau after ~100–200 ms (Fig. 1(b) blue and yellow traces). The presented temperature increases were fairly localized to the illuminated area. Even for small displacements of ~50–100 µm away from the illuminated area, the temperature changes already dropped by ~80%. All recordings were performed at room temperature (~21 °C) and all the IR induced temperature changes were measured with respect to room temperature. The decay of the temperature followed an exponential time course. Instead of using sub-microsecond IR pulses repeated at high frequencies to induce IR inhibition as reported

Biomedical Optics EXPRESS

before [25,28], single IR pulses with durations up to 500 ms were used. The optical power was estimated to be at least 10 times lower, while the optical fiber was 2 to 12 times smaller in core diameter, than those used in previous IR inhibition reports [25–28]. This fiber-power combination resulted in temperature rises were comparable to those reported in previous studies, ~5 to 20 °C [10,25,28]. Due to the high absorption by water in the 2 μm wavelength region, the recorded temperatures presented an upper limit since the exact temperature changes on the axon membrane might be slightly lower than these recorded with an open patch pipette placed slightly above the axon and closer to the IR source. Overall, the open patch pipette provides a close approximation of the amplitude and dynamics of the IR-induced temperature change on the axonal membrane.

2.4. Data analysis

Data acquisition and analysis were performed with Igor Pro (WaveMetrics). Each preparation (N) represented a set of data recorded from an axon dissected from an animal. Statistical results were presented as average the standard error of mean (SEM) and the Student's t-test was used to determine the statistical significance with the significance level α set as 0.05, as specified in the context. Linear interpolation and double-exponential curve fitting were applied to analyze the changes and dynamics of the AP amplitude and duration and temperature transients induced by IR pulses.

3. Results

3.1. Short infrared pulse suppresses action potential amplitude and duration

The effect of a 20 ms IR pulse on neural activities was tested first. AP trains activated by a 1 s current step of 22 nA were compared between trials with (red) and without (blue) illumination from a single IR pulse (Fig. 2(a)). The red bar above the AP trains represents the laser illumination which occurred 100 ms after the onset of the current injection. The gray line underneath the trace marks the timing of the current steps. The average temperature increase induced by such one IR pulse was estimated as 8.7± 0.26 °C (N = 5, see Fig. 1(b)). The IR pulse reduced the amplitude of two APs around the time of IR delivery. The comparison of the AP waveforms on an expanded time scale shows that the AP amplitude and duration were reduced by the IR pulse (Fig. 2(b) top panel). The effects of the IR illumination disappeared ~40 ms after the IR pulse ended and complete recovery of the AP waveform was consistently obtained (Fig. 2(b) bottom panel). The phase plot of the two APs in Fig. 2(b) (top panel) illustrates the decrease in amplitude. The gradual rise around threshold (marked with an arrow) is characteristic for locally induced APs (Fig. 2(c)). To quantify the changes in amplitude and duration, we define the AP amplitude as the difference between the peak and the AP firing threshold (dv/dt= 25 V/s) (Fig. 2(b) lower panel, vertical arrows), and the duration as the full width at half maximum of the AP waveforms (Fig. 2(b) lower panel, horizontal arrows). The averaged reductions in the AP amplitude and duration induced by a 20 ms IR pulse were 3.4 ± 0.06 mV (N = 7, $p = 1 \times 10^{-6}$) and 58 ± 2.9 μs (N = 7, $p = 2 \times 10^{-4}$), respectively (Fig. 2(d)). The various symbols in Fig. 2(d) represent measurements from different preparations. The gray filled symbols represent data collected from preparations without 4-AP treatment. The resting membrane potential and control AP amplitude were monitored continuously in every experiment, as indicators of axonal health. The resting membrane potential and control AP waveforms remained stable for the durations of all experiments, up to 8 hours in some preparations.

3.2. Long infrared pulse blocks locally induced action potentials

In addition to the short IR pulse illumination, the effects of a longer IR pulse (500 ms) on the axonal excitability were also examined to study the dynamics of the AP waveform changes during the rise and fall of the IR induced temperature transients. Representative results with a 500 ms

Biomedical Optics EXPRESS

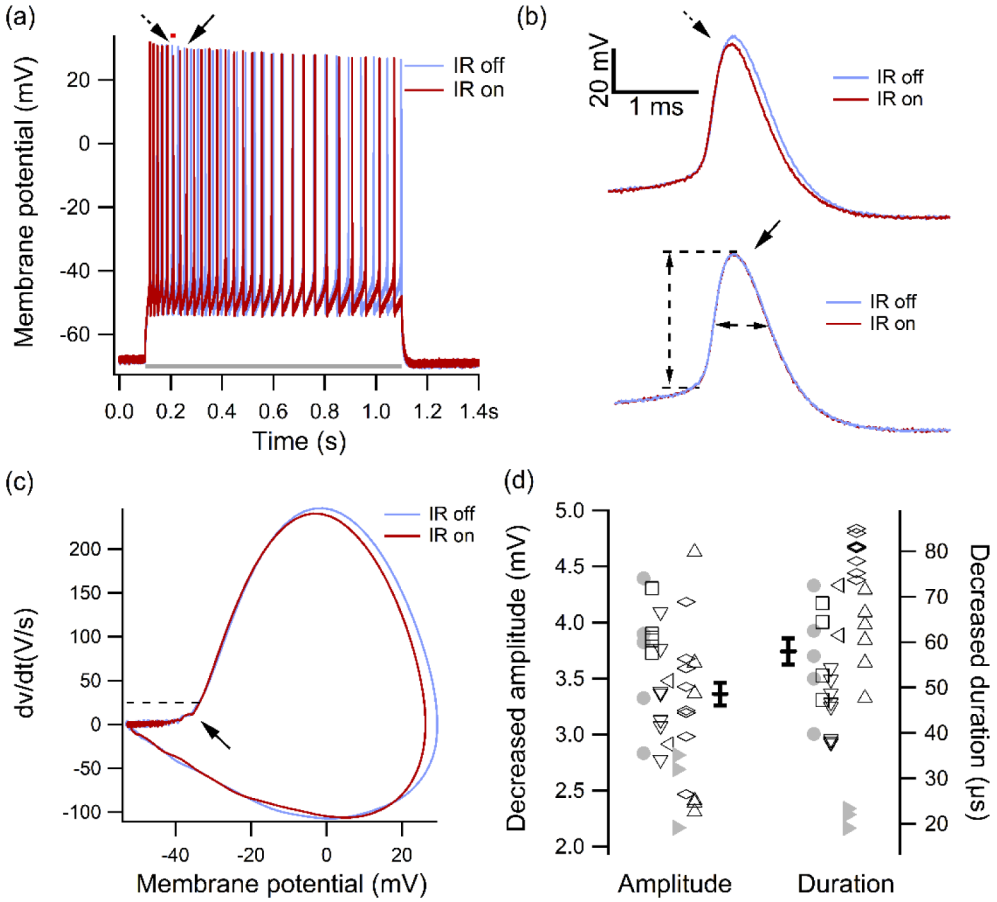

Fig. 2. Impact of 20 ms IR pulses on AP amplitude and duration. (a) Representative AP trains initiated by a 22 nA current step with (red) and without (blue) a 20 ms pulse IR illumination. The red bar above the AP traces indicates the timing (0.2 s to 0.22 s) of the IR pulse. These traces were recorded in the presence of 200 µM 4-AP. The grey line indicates the timing of the current step. The arrows identify APs to be compared in detail in (b). (b) Comparison of AP waveforms on an expanded time scale as indicated by the corresponding arrows in (a) and (b). Top, two APs with and without IR illumination during the 0.2 s to 0.22 s time window. The IR pulse reduced the AP amplitude and duration. Bottom, two APs ~40 ms after the IR pulse. The AP waveform recovered shortly after the IR pulse. The horizontal and vertical arrows in the bottom panel indicate the measurement parameters for AP amplitude and duration measurements. (c) The phase plot of the two APs in (b) top panel shows a reduction in the AP amplitude. The arrow indicates a gradual rise near the point of AP initiation. The dashed line identifies the point where dv/dt = 25 V/s as the threshold of AP initiation. (d) Scatter plot of the IR induced reduction in AP amplitude and duration (N = 7). Each type of symbol represents data from one crayfish preparation. The black symbols represent 4-AP treated preparations while the gray solid symbols illustrate those without 4-AP. The average and standard error of the mean for decreased AP amplitude and duration are highlighted in bold with values of 3.4 ± 0.06 mV and 58 ± 2.9 µs.

Biomedical Optics EXPRESS

IR pulse are shown in Fig. 3. The average temperature rise induced by a 500 ms IR pulse was estimated as 11.8 ± 0.52 °C (N = 5). APs initiated by a current step slightly above the AP firing threshold (16 nA) were inhibited by the IR pulse (Fig. 3(a)). An IR pulse delivered during a higher current step (17 nA) suppressed the AP amplitude at first and then blocked the AP firing for the duration of the IR pulse (Fig. 3(b)). The axon resumed firing after the termination of the IR pulse. An IR pulse delivered during high frequency AP firing (19 nA) caused a progressive decrease in AP amplitude (Fig. 3(c)). Complete recovery was observed ~400 ms after the end of the IR pulse.

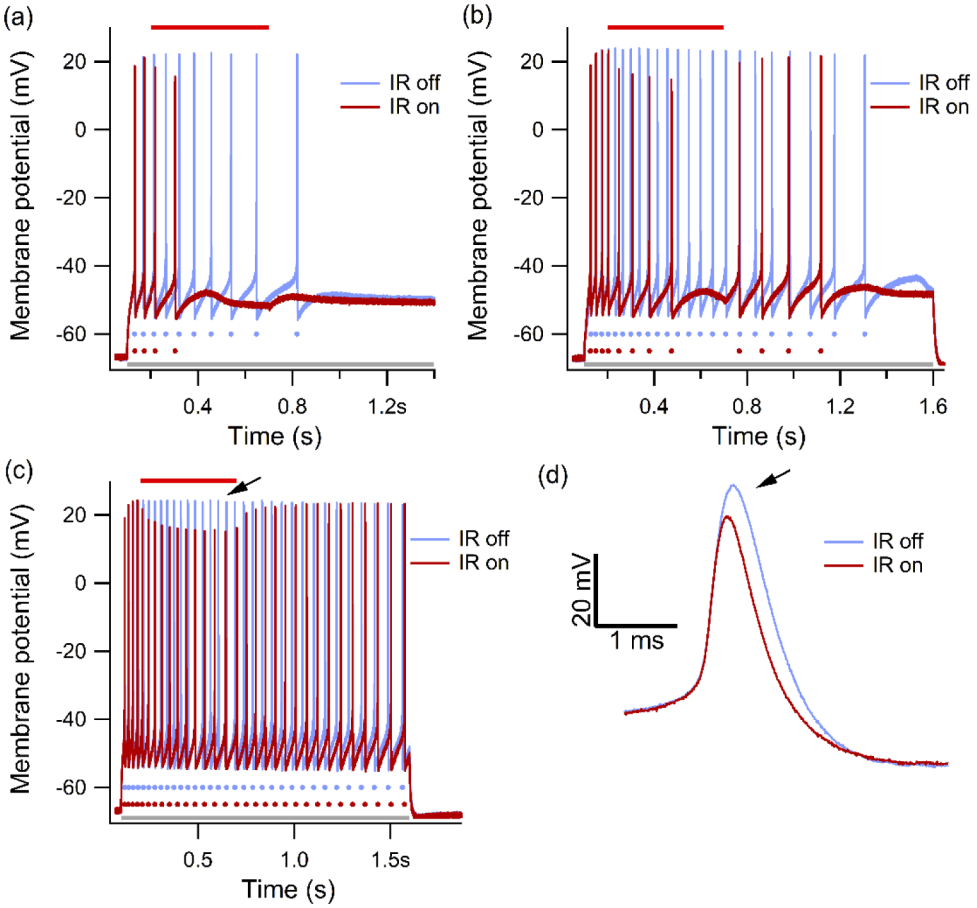

Fig. 3. A 500 ms IR pulse blocked the AP initiation and shaped the AP waveforms. (a) AP trains initiated by a 16 nA step, which was slightly above the firing threshold. The IR pulse completely blocked the APs. (b) AP trains initiated by a 17 nA current step. The AP amplitude and frequency were suppressed before the AP firing was completely inhibited, which recovered after the IR pulse. (c) High firing frequency AP trains from a 19 nA current step. The AP amplitude was progressively decreased by the IR pulse. The red bar above the AP trains indicates the timing of IR pulses (0.2 s to 0.7 s). The grey line illustrates the timing of the current injection. The solid dots under the AP trains represent the AP firing. (d) Comparison of AP waveforms expanded in time with and without the IR pulse. The APs were obtained from a time point close to the end of the IR illumination (arrow in (c)). The IR light reduced AP amplitude and duration. These traces were recorded in the absence of 4-AP.

Biomedical Optics EXPRESS

The AP amplitude reductions and recovery rates with different current steps were comparable, as shown in Figs. 3(b) and 3(c). A comparison of the AP waveforms near the end of the IR pulse (Fig. 3(c) arrow) shows a significant decrease in amplitude (8.7 mV) and duration (124 µs) of the IR illuminated AP. It was also observed that the firing frequency was reduced by the IR pulse, as illustrated by the corresponding dots under the AP trains (Figs. 3(a), (b) and (c)). For the AP trains shown in Fig. 3(c), the instantaneous frequency decreased about 20% near the end of IR illumination. Similar inhibitions in AP initiation and waveform were also observed for IR pulses with durations of 50–200 ms in 8 incidences from five preparations.

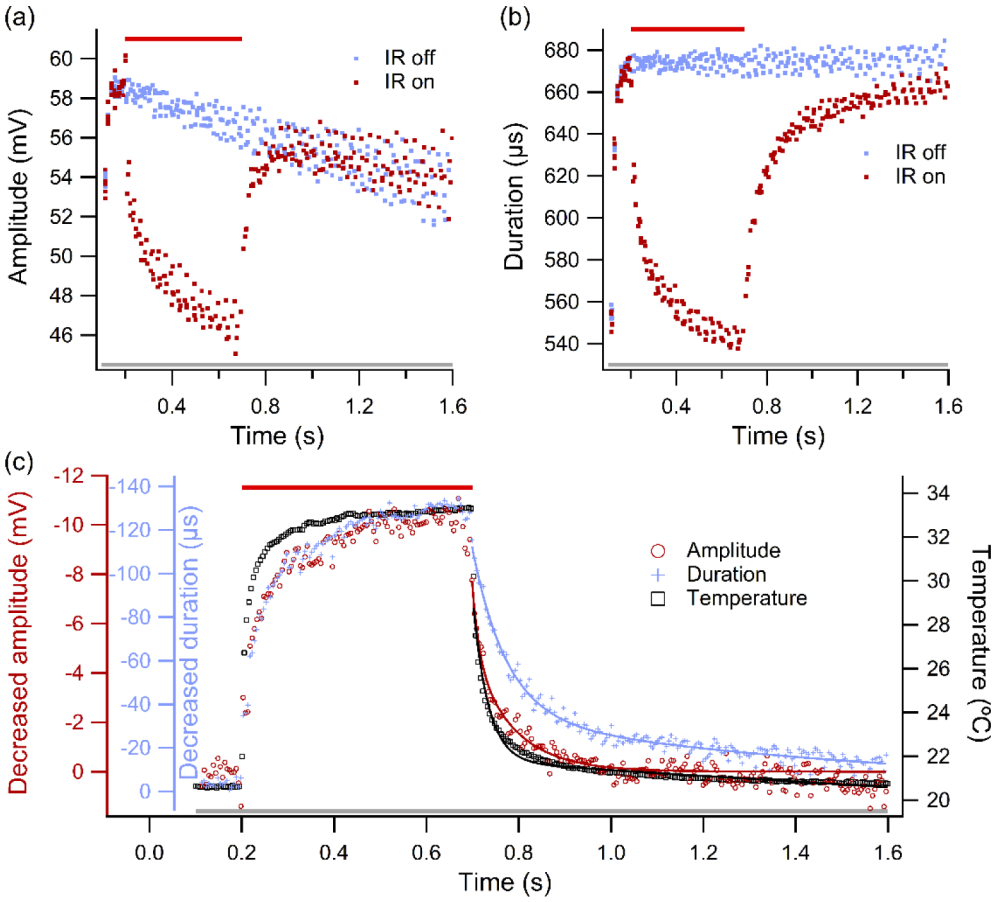

Fig. 4. Dynamics of IR suppression on the AP amplitude and duration evoked by a 21 nA current step. (a), (b) Measured AP amplitude and duration as defined in Fig. 2(b) with and without IR light. Each data point was measured from an AP and plotted against the timing of that AP. The data points were collected from the same preparation based on 5 trials. (c) Comparison of dynamic changes of AP amplitude, duration and temperature. Changes in AP amplitude (duration) were obtained by subtracting data points measured without IR illumination from the amplitude (duration) with IR light. The data after the IR pulse, from 0.7 s to 1.6 s, was fitted with a sum of two decaying exponentials respectively (smooth lines). The amplitude trace (open circle) recovered faster than the duration (cross) after the IR pulse. The red bar above indicates the timing and duration of the IR light. The grey line illustrates the timing and duration of the current injection. These traces were recorded in the absence of 4-AP.

Biomedical Optics EXPRESS

3.3. Dynamics of infrared suppression on action potential amplitude and duration

In order to examine the dynamics of the IR induced suppression, the time course of temperature transients induced by a 500 ms IR pulse was compared with that of AP amplitude and duration changes. To ensure a sufficient time resolution, only trials with continuous firing during the entire period of current injection (1.5 s) and with a firing frequency above 20 Hz were selected for further analysis (e.g. Figure 3(c)). These high frequency trials were repeated 2–10 times in each preparation and the amplitude and duration of every AP were measured. Figure 4(a) displays the amplitude of every AP from 5 trials in one axon. A slight decline in AP amplitude in the absence of the IR light (blue) is noticeable. A 500 ms IR pulse caused a continuous decline in the AP amplitude which rapidly recovered at the end of the IR pulse (red). The AP duration exhibited a relatively flat trajectory under control conditions (Fig. 4(b), blue) and was largely reduced during IR illumination (Fig. 4(b), red). The recovery of the AP duration at the end of the IR pulse was slower than that of the AP amplitude.

In order to facilitate the comparison between the time courses of temperature transients and those of AP parameters, the IR induced changes in AP amplitude ($\Delta\, AP_{amplitude}$) and duration ($\Delta\, AP_{duration}$) were isolated, by subtracting the parameters measured in the absence of IR illumination from those with the IR pulse. The isolated amplitude and duration differences are plotted on the same time scale as that of temperature transients (Fig. 4(c)). Although there may be subtle difference in $\Delta\, AP_{amplitude}$ and $\Delta\, AP_{duration}$ during the IR pulse illumination, the main difference between these two parameters is during the return phase after the IR pulse was terminated. The $\Delta\, AP_{amplitude}$ exhibited a faster return compared to $\Delta\, AP_{duration}$. To quantitatively verify the difference in decay, we used a sum of two exponential functions with a fast and a slow time constant τ_1 and τ_2 to fit the recovery phases of amplitude, duration and temperature (see smooth lines in Fig. 4(c)). $\Delta\, AP_{amplitude}$ consistently displayed a faster decay time constant in the first of the two decay components. The ratio of the first decay time constant between $\Delta\, AP_{duration}$ and $\Delta\, AP_{amplitude}$ was 3.8 ± 0.74 ($N = 5$, $p = 0.009$)**.** Similar trends were observed for shorter IR pulse durations (e.g. 200 ms).

3.4. Infrared pulse reduces the input resistance

Since an IR pulse consistently generates a slight reduction in membrane potential during subthreshold depolarization and hyperpolarization, the impact of the IR illumination on the input resistance (R_{in}) was examined. The R_{in} is determined by the membrane resistance and axoplasmic resistance, where the former is generally considered dominant. The R_{in} was calculated from the slope of the *V-I* plot. Figure 5(a) shows a small reduction in the membrane voltage for a single 500 ms IR pulse during both hyperpolarization and subthreshold depolarization, which suggests a decrease in the R_{in} induced by IR illumination. The average membrane potential changes that occurred during the last 20 ms of the applied IR pulse are plotted against the current injection amplitudes (Fig. 5(b)). The membrane potential measured in the absence of an IR pulse was obtained from the same time window as that with an IR pulse. Each data point was averaged over 5–10 trials. The linear fits illustrate the decrease in R_{in} (slope) and a slight shift of the reversal potential towards the more negative direction. The average decrease in R_{in} from eight preparations is 8.8% ± 0.65% ($N = 8$, $p = 3 \times 10^{-6}$).

Biomedical Optics EXPRESS

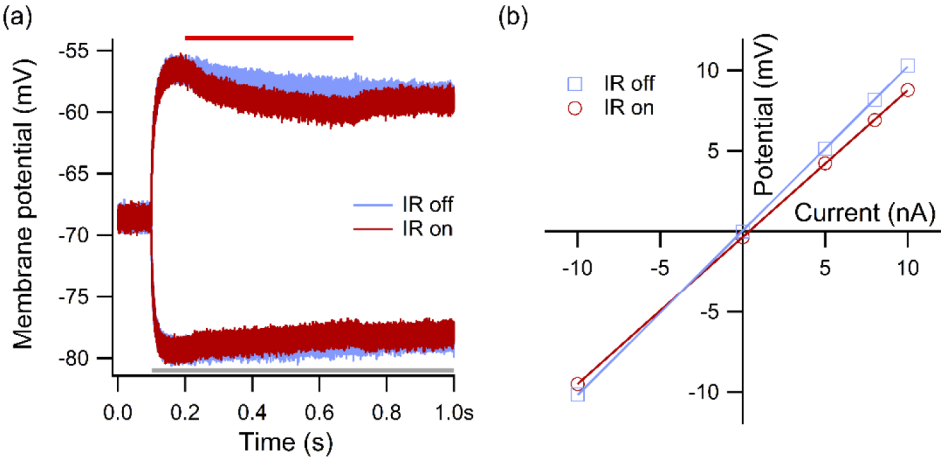

Fig. 5. Effect of a 500 ms IR pulse on the input resistance. (a) The IR pulse decreases the membrane voltage deflections during both hyperpolarization and subthreshold depolarization. The red bar above indicates the timing of the IR light. The grey line illustrates the timing and duration of the current injection. (b) The average membrane potentials with and without IR pulse recorded between 0.68 s and 0.7 s (last 20 ms of IR illumination) are plotted against the corresponding current injection steps. Linear fitting shows the decrease in slope with IR pulses. Each data point was averaged over 5–10 trials.

4. Discussion

In this report, we used the TECC on the unmyelinated motor axon of the crayfish opener preparation to investigate the effects of a 2 μm IR laser pulse on axonal excitability and AP waveform. We found that the IR pulses delivered to a small region of the axon could inhibit the initiation of APs and reduce the amplitude and duration of initiated APs. The presented intracellular recordings provide an unambiguous interpretation of the intracellular events mediated by the IR illumination. Specifically, at the threshold level of depolarization, IR light could inhibit the AP initiation. For suprathreshold electrical stimulation, the IR pulse reduced the AP amplitude and duration. Modulations on the AP firing frequency were also observed. Changes in $\Delta AP_{amplitude}$ and $\Delta AP_{duration}$ during 500 ms IR pulses exhibited similar time courses. However, the recovery of these parameters upon the termination of the IR pulses diverged, with $\Delta AP_{amplitude}$ decaying significantly faster than $\Delta AP_{duration}$. An 8.8% reduction in R_{in} was detected during the IR illumination, suggesting a temperature dependent decrease in the membrane resistance, which could contribute to the inhibition reported here. However, as the IR light induced local temperature increase is not insignificant (8–12 °C), we believe that temperature dependent changes in Na^+ and K^+ channel kinetics may also play a significant role in the IR induced inhibition and AP waveform modulation. Mechanisms and implications underlying these observations reported here are discussed further below.

4.1. *Mechanisms underlying infrared induced inhibition and action potential waveform modulation*

Among various biophysical mechanisms proposed by IR nerve stimulation studies (see introduction), the photothermal effects have been considered as the dominant parameter underlying IR modulation of nerve activity and excitability [9]. Other potential processes, photochemical, photomechanical, and photoacoustic mechanisms for example, usually require high photon energy or are associated with specific neural preparations. These phenomena have been discussed in detail [6]. Base on the pulse durations combined with low power used in this report, they are

Biomedical Optics EXPRESS

unlikely to play a role in our observations. Thus, we will focus the discussion here on the thermal transient effects that can implicate the ion channels and axonal membrane.

A previous study using squid giant axons demonstrated that changes in steady state bath temperature profoundly altered the AP duration and amplitude [33]. A recent study using unmyelinated axons in the rat cerebellum and hippocampus showed that raising bath temperature reduced or blocked CAPs [39]. In general, the AP amplitude and duration decreased when the bath temperature was raised. In a voltage clamp study of the frog myelinated axon, it was concluded that the reduction of AP amplitude in response to rising temperatures could be attributed to the higher Q_{10} values of the rate constants of K^+ channel activation and Na^+ channel inactivation compared to those of Na^+ channel activation. A recent experimental and simulation study with mouse cortical neurons confirmed that the decreases in AP amplitude and duration at higher temperatures were mainly due to an increased rate of Na^+ channel inactivation [40]. However, an accelerated K^+ channel activation was suggested to be the primary cause of the thermal inhibition of APs in a simulation study based on the squid giant axon [35]. In line with these studies, the temperature dependent changes in channel kinetics can explain the reduction in AP amplitude and duration during IR illumination reported here. Specifically, the non-uniform temperature sensitivities of these rate constants suggest that, during the IR pulse induced local temperature transients, the Na^+ influx during the rising phase of an AP was weakened by the faster Na^+ channel inactivation while the accelerated Na^+ channel inactivation together with the sped-up of K^+ channel activation hastened the falling phase.

The use of 500 ms IR pulses offered an opportunity to examine the dynamics of the IR nerve inhibition. Specifically, we followed the changes in AP amplitude and duration, as $\Delta\, AP_{amplitude}$ and $\Delta\, AP_{duration}$, during and after IR illumination. While the $\Delta\, AP_{amplitude}$ and $\Delta\, AP_{duration}$ rose in parallel during the IR pulses, these parameters exhibited different dynamics after the termination of IR pulse, as $\Delta\, AP_{amplitude}$ decayed significantly faster than $\Delta\, AP_{duration}$. This was consistently observed in 5 preparations, 3/5 with 200 μM 4-AP treatment and 2/5 without. The interplay among the temperature dependent Na^+ and K^+ channel kinetics could be responsible for the different rates of decay. The absolute AP amplitude in crayfish is mainly determined by the Na^+ and 4-AP sensitive K^+ channels [36]. Since the difference in the recovery rates between the $\Delta\, AP_{amplitude}$ and $\Delta\, AP_{duration}$ was observed both with and without 4-AP, the fast recovery of the $\Delta\, AP_{amplitude}$ is more likely to reflect the behavior of Na^+ channel kinetics. In fact, the rate of the $\Delta\, AP_{amplitude}$ recovery closely followed that of the temperature transients induced by the IR pulse (Fig. 4(c)). To interpret the slower recovery of the AP duration, it needs to be taken into consideration that both Na^+ channel inactivation and K^+ channel activation play a role in shaping the AP duration. Their roles in shaping $\Delta\, AP_{duration}$ recovery remain to be evaluated by simulation studies. In addition to the channel kinetics, the morphology of the axon and the charge redistribution along the axon should also be considered. Since the IR illumination is limited to a small segment of the axon, APs from the nearby axonal regions that were not exposed to the IR pulses, and experienced lower and slower temperature rises, should have more "normal" waveforms. These "neighboring" APs, as they propagated away from the illuminated area, may also impact the falling phase of the recorded APs. Explaining the trajectories of the $\Delta\, AP_{amplitude}$ and $\Delta\, AP_{duration}$ during and after the IR pulse would benefit from the spatial mapping of AP waveforms and temperature transients as well as the modeling studies that incorporate both the temperature dependence of channel kinetics and cable properties of the axon.

The examination of IR-induced subthreshold events shed light on potential contributions of phenomena associated with transient temperature changes and that can affect any transient IR mediated neural modulation. To the best of our knowledge, there have been no reports of transient receptor potential vanilloid (TRPV) channels in the inhibitory motor axon of crayfish. In addition, since the IR light did not induce significant depolarization (Fig. 5(a)), as would be typically expected from the TRPV channels [41,42], this class of ion channels is unlikely to play

Biomedical Optics EXPRESS

a role in the results shown here. Further, it has been suggested that IR irradiation of the cell membrane can generate capacitive currents which in turn can influence the membrane potential [10–13]. However, membrane potential changes associated with IR mediated capacitive currents typically exhibit a rapid rising phase at the onset of the IR irradiation, which was not observed here (Fig. 5(a)). Therefore, we believe that any potential membrane capacitance changes due to IR illumination are minimal to the IR-mediated inhibition in our experimental configuration. While calcium channel kinetics in theory can also be altered by temperature transients, they are not really relevant in our study because previous imaging studies established that Ca^{2+} channels in crayfish axons are localized in terminal varicosities and not in the main axonal branches [43]. Although there is a large body of studies documenting IR induced release of Ca^{2+} from intracellular stores [14,16,44–46], this process is unlikely to be related to our results since the AP waveform changes reported here recovered within 50–500 ms, while the intracellular Ca^{2+} release process in general occurs over a time scale of seconds.

In addition to affecting channel kinetics, raising the bath temperature in steady state is also known to increase the membrane permeability [34]. A study using Chinese hamster ovarian cells showed that the membrane fluidity increased with IR pulse exposure [47], which could be the mechanism underlying the IR induced reduction in R_{in} (Fig. 5). It is reasonable to suggest that the reversible blocking of the AP initiation at threshold level current steps, as shown in Figs. 3(a) and (b), could be attributed to the IR induced reduction in the membrane resistance. However, it is unclear how much the R_{in} reduction contributed to the AP waveform modulations during suprathreshold current stimulation (Figs. 1(a) and 3(c)). Since the sizes of the axon are about 10 mm in length and 30 μm in diameter, the 50 μm optical fiber used in this work illuminated less than 1% of the axon surface membrane. Simulation studies that incorporate passive membrane parameters and channel kinetics will be needed to determine whether the small resistance decrease in such a localized area is sufficient to generate the inhibition at threshold current injection levels reported here.

4.2. Comparison with previous studies and implications

In the investigation of IR mediated neuronal inhibition, the majority of previous studies used extracellular recordings such as single unit recordings, CAPs measurement, or imaging techniques to document the impact of IR illumination. Intracellular recordings reported here contribute important insights to previous studies. The observation that IR pulses reduced the amplitude and duration of APs activated by suprathreshold current steps is relevant to results showing reduction in CAPs [25]. Specifically, CAPs measured from vertebrate peripheral nerves were mainly observed in myelinated axons. Since these axons typically have large safety factors [48], propagating APs initiated by large charging currents in these axons are equivalent to the APs evoked by the suprathreshold current injections reported here. Therefore, reduced CAPs during IR illumination could be due to a reduction in AP amplitude and duration in some of the axons, rather than complete AP propagating failures in a subset of the axons. Since the propagating APs with reduced amplitudes and durations may recover after passing IR illuminated areas [32,35], intended functional consequences of reduced CAPs may not be achievable.

We also demonstrated that the AP initiation could be blocked with current injection steps around the threshold level. A simulation study suggested that the temperature rise needed to block AP initiation was significantly lower than that required to block propagating APs [32]. It is likely that higher temperature transients could block the APs initiated by suprathreshold current injections in our preparation. In fact, a modeling study based on the squid giant axon indicated that, in order for a localized temperature rise to block conducting APs, the temperature rise should be around 20 °C [35], which was significantly higher than the ~12 °C temperature rise above room temperature reported here.

Biomedical Optics EXPRESS

It is worth noting that a delicate balance exists with regards to the application of IR nerve inhibition, since using IR illumination schemes that are sufficiently strong to block propagating APs may not be physiologically desirable. Meanwhile, reduced AP amplitude and duration that are induced by physiologically tolerable IR illumination levels can potentially recover after propagating a certain distance along the axon. A detailed mechanistic understanding of the IR mediated inhibition combined with optimizing the efficiency of IR nerve inhibition and lowering the temperature rises by adapting new IR illumination regimes or combining different nerve modulation approaches will be important for any therapeutic applications.

5. Conclusion

We used intracellular recordings from the crayfish unmyelinated motor axons to study the effects of 2 μm IR light on AP initiation and waveform modulation. Results reported here showed that temperature-dependent Na^+ and K^+ channel kinetics and membrane resistance can contribute to the IR inhibition of neural activities. It was observed for the first time that the AP amplitude and duration recovered at different rates, after the IR pulse ended. This marks an interesting finding that can fuel further studies about the underlying mechanisms. The measured changes in the AP waveform and in the input resistance based on intracellular measurements can guide future modeling studies on the biophysics of IR nerve modulation. In summary, observations reported here provide valuable insights for future implementations of IR light related technology for basic research and clinical applications.

Funding

Air Force Office of Scientific Research (FA9550-17-1-0276).

Acknowledgements

We would like to thank Feiyuan Yu for helping with the crayfish preparations.

Disclosures

The authors declare no conflicts of interests.

References

1. J. Wells, C. Kao, K. Mariappan, J. Albea, E. D. Jansen, P. Konrad, and A. Mahadevan-Jansen, "Optical stimulation of neural tissue in vivo," Opt. Lett. **30**(5), 504 (2005).
2. J. Wells, C. Kao, E. D. Jansen, P. Konrad, and A. Mahadevan-Jansen, "Application of infrared light for in vivo neural stimulation," J. Biomed. Opt. **10**(6), 064003 (2005).
3. N. I. Smith, Y. Kumamoto, S. Iwanaga, J. Ando, K. Fujita, and S. Kawata, "A femtosecond laser pacemaker for heart muscle cells," Opt. Express **16**(12), 8604 (2008).
4. M. W. Jenkins, A. R. Duke, S. Gu, Y. Doughman, H. J. Chiel, H. Fujioka, M. Watanabe, E. D. Jansen, and A. M. Rollins, "Optical pacing of the embryonic heart," Nat. Photonics **4**(9), 623–626 (2010).
5. C.-P. Richter, A. I. Matic, J. D. Wells, E. D. Jansen, and J. T. Walsh, "Neural stimulation with optical radiation," Laser Photonics Rev. **5**(1), 68–80 (2011).
6. C.-P. Richter and X. Tan, "Photons and neurons," Hear. Res. **311**, 72–88 (2014).
7. M. Chernov and A. W. Roe, "Infrared neural stimulation: a new stimulation tool for central nervous system applications," Neurophotonics **1**(1), 011011 (2014).
8. J. Wells, P. Konrad, C. Kao, E. D. Jansen, and A. Mahadevan-Jansen, "Pulsed laser versus electrical energy for peripheral nerve stimulation," J. Neurosci. Methods **163**(2), 326–337 (2007).
9. J. Wells, C. Kao, P. Konrad, T. Milner, J. Kim, A. Mahadevan-Jansen, and E. D. Jansen, "Biophysical Mechanisms of Transient Optical Stimulation of Peripheral Nerve," Biophys. J. **93**(7), 2567–2580 (2007).
10. M. G. Shapiro, K. Homma, S. Villarreal, C.-P. Richter, and F. Bezanilla, "Infrared light excites cells by changing their electrical capacitance," Nat. Commun. **3**(1), 736 (2012).
11. Q. Liu, M. J. Frerck, H. A. Holman, E. M. Jorgensen, and R. D. Rabbitt, "Exciting Cell Membranes with a Blustering Heat Shock," Biophys. J. **106**(8), 1570–1577 (2014).

Biomedical Optics EXPRESS

12. M. Plaksin, E. Kimmel, and S. Shoham, "Correspondence: Revisiting the theoretical cell membrane thermal capacitance response," Nat. Commun. **8**(1), 1431 (2017).
13. M. Plaksin, E. Shapira, E. Kimmel, and S. Shoham, "Thermal Transients Excite Neurons through Universal Intramembrane Mechanoelectrical Effects," Phys. Rev. X **8**(1), 011043 (2018).
14. G. M. Dittami, S. M. Rajguru, R. A. Lasher, R. W. Hitchcock, and R. D. Rabbitt, "Intracellular calcium transients evoked by pulsed infrared radiation in neonatal cardiomyocytes," J. Physiol. **589**(6), 1295–1306 (2011).
15. J. M. Cayce, M. B. Bouchard, M. M. Chernov, B. R. Chen, L. E. Grosberg, E. D. Jansen, E. M. C. Hillman, and A. Mahadevan-Jansen, "Calcium imaging of infrared-stimulated activity in rodent brain," Cell Calcium **55**(4), 183–190 (2014).
16. V. Lumbreras, E. Bas, C. Gupta, and S. M. Rajguru, "Pulsed infrared radiation excites cultured neonatal spiral and vestibular ganglion neurons by modulating mitochondrial calcium cycling," J. Neurophysiol. **112**(6), 1246–1255 (2014).
17. E. S. Albert, J. M. Bec, G. Desmadryl, K. Chekroud, C. Travo, S. Gaboyard, F. Bardin, I. Marc, M. Dumas, G. Lenaers, C. Hamel, A. Muller, and C. Chabbert, "TRPV4 channels mediate the infrared laser-evoked response in sensory neurons," J. Neurophysiol. **107**(12), 3227–3234 (2012).
18. H. T. Beier, G. P. Tolstykh, J. D. Musick, R. J. Thomas, and B. L. Ibey, "Plasma membrane nanoporation as a possible mechanism behind infrared excitation of cells," J. Neural Eng. **11**(6), 066006 (2014).
19. M. Schultz, P. Baumhoff, H. Maier, I. U. Teudt, A. Krüger, T. Lenarz, and A. Kral, "Nanosecond laser pulse stimulation of the inner ear-a wavelength study," Biomed. Opt. Express **3**(12), 3332–3345 (2012).
20. A. Rettenmaier, T. Lenarz, and G. Reuter, "Nanosecond laser pulse stimulation of spiral ganglion neurons and model cells," Biomed. Opt. Express **5**(4), 1014 (2014).
21. H.-J. Feng, C. Kao, M. J. Gallagher, E. D. Jansen, A. Mahadevan-Jansen, P. E. Konrad, and R. L. Macdonald, "Alteration of GABAergic neurotransmission by pulsed infrared laser stimulation," J. Neurosci. Methods **192**(1), 110–114 (2010).
22. J. M. Cayce, R. M. Friedman, E. D. Jansen, A. Mahavaden-Jansen, and A. W. Roe, "Pulsed infrared light alters neural activity in rat somatosensory cortex in vivo," NeuroImage **57**(1), 155–166 (2011).
23. E. J. Peterson and D. J. Tyler, "Motor neuron activation in peripheral nerves using infrared neural stimulation," J. Neural Eng. **11**(1), 016001 (2014).
24. J. M. Cayce, R. M. Friedman, G. Chen, E. D. Jansen, A. Mahadevan-Jansen, and A. W. Roe, "Infrared neural stimulation of primary visual cortex in non-human primates," NeuroImage **84**, 181–190 (2014).
25. A. R. Duke, M. W. Jenkins, H. Lu, J. M. McManus, H. J. Chiel, and E. D. Jansen, "Transient and selective suppression of neural activity with infrared light," Sci. Rep. **3**(1), 2600 (2013).
26. A. J. Walsh, G. P. Tolstykh, S. Martens, B. L. Ibey, and H. T. Beier, "Action potential block in neurons by infrared light," Neurophotonics **3**(4), 040501 (2016).
27. Y. T. Wang, A. M. Rollins, and M. W. Jenkins, "Infrared inhibition of embryonic hearts," J. Biomed. Opt. **21**(6), 060505 (2016).
28. E. H. Lothet, K. M. Shaw, H. Lu, J. Zhuo, Y. T. Wang, S. Gu, D. B. Stolz, E. D. Jansen, C. C. Horn, H. J. Chiel, and M. W. Jenkins, "Selective inhibition of small-diameter axons using infrared light," Sci. Rep. **7**(1), 3275 (2017).
29. X. Zhu, J.-W. Lin, and M. Y. Sander, "Infrared block of Na+ and Ca2+ spikes in in crayfish neuromuscular junction," Proc. SPIE **10866**, 108660E (2019).
30. Q. Xia and T. Nyberg, "Inhibition of cortical neural networks using infrared laser," J. Biophotonics **12**(7), e201800403 (2019).
31. A. R. Duke, H. Lu, M. W. Jenkins, H. J. Chiel, and E. D. Jansen, "Spatial and temporal variability in response to hybrid electro-optical stimulation," J. Neural Eng. **9**(3), 036003 (2012).
32. Z. Mou, I. F. Triantis, V. M. Woods, C. Toumazou, and K. Nikolic, "A Simulation Study of the Combined Thermoelectric Extracellular Stimulation of the Sciatic Nerve of the Xenopus Laevis: The Localized Transient Heat Block," IEEE Trans. Biomed. Eng. **59**(6), 1758–1769 (2012).
33. A. L. Hodgkin and B. Katz, "The effect of temperature on the electrical activity of the giant axon of the squid," J. Physiol. **109**(1-2), 240–249 (1949).
34. A. F. Huxley, "Ion movements during nerve activity," Ann. N. Y. Acad. Sci. **81**(2), 221–246 (1959).
35. M. Ganguly, M. W. Jenkins, E. D. Jansen, and H. J. Chiel, "Thermal block of action potentials is primarily due to voltage-dependent potassium currents: a modeling study," J. Neural Eng. **16**(3), 036020 (2019).
36. J.-W. Lin, "Spatial variation in membrane excitability modulated by 4-AP-sensitive K^+ channels in the axons of the crayfish neuromuscular junction," J. Neurophysiol. **107**(10), 2692–2702 (2012).
37. D. M. Wieliczka, S. Weng, and M. R. Querry, "Wedge shaped cell for highly absorbent liquids: infrared optical constants of water," Appl. Opt. **28**(9), 1714 (1989).
38. J. Yao, B. Liu, and F. Qin, "Rapid Temperature Jump by Infrared Diode Laser Irradiation for Patch-Clamp Studies," Biophys. J. **96**(9), 3611–3619 (2009).
39. D. Pekala, H. Szkudlarek, and M. Raastad, "Typical gray matter axons in mammalian brain fail to conduct action potentials faithfully at fever-like temperatures," Physiol Rep **4**(19), e12981 (2016).
40. Y. Yu, A. P. Hill, and D. A. McCormick, "Warm Body Temperature Facilitates Energy Efficient Cortical Action Potentials," PLoS Comput. Biol. **8**(4), e1002456 (2012).

Biomedical Optics EXPRESS

41. C. Montell, "Physiology, phylogeny, and functions of the TRP superfamily of cation channels," Sci. STKE **2001**(90), re1 (2001).
42. H. Li, "TRP channel classification," in *Advances in Experimental Medicine and Biology* (Springer New York LLC, 2017), Vol. 976, pp. 1–8.
43. K. Delaney, D. W. Tank, and R. S. Zucker, "Presynaptic calcium and serotonin-mediated enhancement of transmitter release at crayfish neuromuscular junction," J. Neurosci. **11**(9), 2631–2643 (1991).
44. J. N. Barrett, S. Rincon, J. Singh, C. Matthewman, J. Pasos, E. F. Barrett, and S. M. Rajguru, "Pulsed infrared releases ca2+ from the endoplasmic reticulum of cultured spiral ganglion neurons," J. Neurophysiol. **120**(2), 509–524 (2018).
45. D. Moreau, C. Lefort, J. Pas, S. M. Bardet, P. Leveque, and R. P. O'Connor, "Infrared neural stimulation induces intracellular Ca $^{2+}$ release mediated by phospholipase C," J. Biophotonics **11**(2), e201700020 (2018).
46. A. Y. Rhee, G. Li, J. Wells, and J. P. Y. Kao, "Photostimulation of sensory neurons of the rat vagus nerve," in S. L. Jacques, W. P. Roach, and R. J. Thomas, eds. (2008), p. 68540E.
47. A. J. Walsh, J. C. Cantu, B. L. Ibey, and H. T. Beier, "Short infrared laser pulses increase cell membrane fluidity," Proc. SPIE **10062**, 100620D (2017).
48. H. Bostock and P. Grafe, "Activity-dependent excitability changes in normal and demyelinated rat spinal root axons," J. Physiol. **365**(1), 239–257 (1985).